Title

Calcium Binding Rigidifies the C2 Domain and the Intradomain Interaction of GIVA Phospholipase A2 as Revealed by Hydrogen/Deuterium Exchange Mass Spectrometry*

Journal

Journal of Biological Chemistry, 283(15)

ISSN

0021-9258

Authors

Hsu, Yuan-Hao
Burke, John E
Stephens, Daren L
et al.

Publication Date

2008-04-01

DOI

10.1074/jbc.m708143200

Peer reviewed

THE JOURNAL OF BIOLOGICAL CHEMISTRY VOL. 283, NO. 15, pp. 9820–9827, April 11, 2008

Calcium Binding Rigidifies the C2 Domain and the Intradomain Interaction of GIVA Phospholipase A_2 as Revealed by Hydrogen/Deuterium Exchange Mass Spectrometry*

Received for publication, October 1, 2007, and in revised form, December 31, 2007 Published, JBC Papers in Press, January 21, 2008, DOI 10.1074/jbc.M708143200

Yuan-Hao Hsu[‡§], John E. Burke[‡§], Daren L. Stephens[‡§], Raymond A. Deems[‡§], Sheng Li[¶], Kyle M. Asmus[¶], Virgil L. Woods, Jr.[¶1], and Edward A. Dennis[‡§2]

From the Departments of [‡]Chemistry and Biochemistry, [§]Pharmacology, and [¶]Medicine and the Biomedical Sciences Graduate Program, University of California, San Diego, La Jolla, California 92093-0601

The GIVA phospholipase A_2 (PLA_2) contains two domains: a calcium-binding domain (C2) and a catalytic domain. These domains are linked via a flexible tether. GIVA PLA_2 activity is Ca^{2+}-dependent in that calcium binding promotes protein docking to the phospholipid membrane. In addition, the catalytic domain has a lid that covers the active site, presumably regulating GIVA PLA_2 activity. We now present studies that explore the dynamics and conformational changes of this enzyme in solution utilizing peptide amide hydrogen/deuterium (H/D) exchange coupled with liquid chromatography-mass spectrometry (DXMS) to probe the solvent accessibility and backbone flexibility of the C2 domain, the catalytic domain, and the intact GIVA PLA_2. We also analyzed the changes in H/D exchange of the intact GIVA PLA_2 upon Ca^{2+} binding. The DXMS results showed a fast H/D-exchanging lid and a slow exchanging central core. The C2 domain showed two distinct regions: a fast exchanging region facing away from the catalytic domain and a slow exchanging region present in the "cleft" region between the C2 and catalytic domains. The slow exchanging region of the C2 domain is in tight proximity to the catalytic domain. The effects of Ca^{2+} binding on GIVA PLA_2 are localized in the C2 domain and suggest that binding of two distinct Ca^{2+} ions causes tightening up of the regions that surround the anion hole at the tip of the C2 domain. This conformational change may be the initial step in GIVA PLA_2 activation.

The cytosolic group IVA (GIVA)[3] phospholipase A_2 (PLA_2), also known as $cPLA_2$, was purified and cloned in 1991 (1, 2). It is one of the few phospholipases in the phospholipase A_2 superfamily shown to be important in lipid mediator biosynthesis (3, 4). GIVA PLA_2 hydrolyzes membrane phospholipids at the *sn*-2 position to release free arachidonic acid, which is the precursor of numerous eicosanoids including the prostaglandins and leukotrienes (5, 6) involved in the inflammatory and pain response (7–9). Understanding the regulation of the catalytic activity of GIVA PLA_2 is crucial for understanding eicosanoid metabolism.

The activity of the 85-kDa GIVA PLA_2 has been suggested to be regulated by several factors including the intracellular Ca^{2+} concentration, its phosphorylation state, and the binding of various activators. Since the GIVA PLA_2 was discovered in 1986, the activity of this enzyme has been known to be Ca^{2+}-dependent (10, 11). The Ca^{2+}-dependent lipid-binding domain (C2 domain) at the N terminus, which is linked to a catalytic domain where phospholipid hydrolysis occurs, was later identified (12). Further studies of the GIVA PLA_2 activity showed up-regulation by p38 protein kinase mainly through Ser-505 phosphorylation (13–15). Various membrane-associated activators have been shown to bind to GIVA PLA_2 and upregulate its activity. In particular, we have shown that the membrane-associated phosphatidylinositol 4,5-bisphosphate can bind to the "lysine pocket" of GIVA PLA_2 with high affinity and specificity to activate the GIVA PLA_2 independent of Ca^{2+} (16, 17). Another membrane-associated activator, ceramide 1-phosphate, has been shown to bind to the cation groove of the C2 domain to activate GIVA PLA_2 in a Ca^{2+}-dependent manner (18, 19).

Calcium binding is crucial for GIVA PLA_2 activation. Two calcium ions coordinate with the calcium-binding loops, CBL1, CBL2, and CBL3, in the C2 domain, which is illustrated in known C2 domain structures (20–22). These two Ca^{2+} ions neutralize the negative charge in the anion hole to facilitate the C2 domain's hydrophobic interaction with phospholipid membranes (21, 22). Various models of membrane penetration for the GIVA PLA_2 have been proposed to explain the hydrolysis activity of GIVA PLA_2 (23, 24). However, the x-ray crystal structure cannot fit the model perfectly unless there is a slight twist of the catalytic domain. Intradomain interactions may change the position of the C2 domain relative to the catalytic domain from that assumed in the crystal structure interpretation. Also, structural information regarding the calcium-free form of GIVA PLA_2 is limited, because its NMR and x-ray crys-

* This work was supported in part by National Institutes of Health Grants GM20501(to E. A. D.) and CA099835, CA118595, GM037684, AI0220221, and AI022160 (to V. L. W.) and Discovery Grant UC10591 from the University of California Industry-University Cooperative Research Program (to V. L. W.). The costs of publication of this article were defrayed in part by the payment of page charges. This article must therefore be hereby marked "*advertisement*" in accordance with 18 U.S.C. Section 1734 solely to indicate this fact.

[1] To whom correspondence may be addressed. Tel.: 858-534-2180; Fax: 858-534-2606; E-mail: vwoods@ucsd.edu.

[2] To whom correspondence may be addressed. Tel.: 858-534-3055; Fax: 858-534-7390; E-mail: edennis@ucsd.edu.

[3] The abbreviations used are: GIVA, group IVA; PLA_2, phospholipase A_2; DXMS, hydrogen/deuterium exchange coupled with liquid chromatography-mass spectrometry; H/D, hydrogen/deuterium.

tal structure are not available. It is necessary to analyze the entire GIVA PLA_2 and especially its intradomain interactions to fully understand the regulation of GIVA PLA_2.

Peptide amide hydrogen/deuterium exchange coupled with liquid chromatography mass spectrometry (DXMS) has been widely used to analyze the interface of protein-protein interactions (25, 26), protein conformational changes (27, 28), and protein dynamics (29, 30). The present study represents the first attempt to use DXMS to study intradomain interactions and the Ca^{2+} binding effect on the GIVA PLA_2. This technique should complement what can be learned from NMR and x-ray crystallographic analysis. Our results describe the intradomain interactions between the C2 domain and the catalytic domain and confirm that the major conformational responses to Ca^{2+} are localized to the calcium-binding loop of the C2 domain. A tightened conformation of the C2 domain appears upon Ca^{2+} binding. Herein, we explore the resultant effects on the catalytic domain.

EXPERIMENTAL PROCEDURES

Materials—All reagents were analytical reagent grade or better.

Protein Expression and Purification—C-terminal His_6-tagged GIVA PLA_2, the C2 domain, and the catalytic domain were expressed using recombinant baculovirus in a suspension culture of Sf9 insect cells (16). The cell pellet was lysed in 25 mM Tris-HCl, pH 8.0, 150 mM NaCl, 2 mM β-mercaptoethanol, and 2 mM EGTA, and then the insoluble portion was removed by centrifugation at 12,000 $\times$ *g* for 30 min. The supernatant was passed through a column comprised of 6 ml of nickel-nitrilotriacetic acid-agarose (Qiagen, Valencia, CA). The protein in the native state was eluted in the "protein buffer" (25 mM Tris-HCl, pH 8.0, 100 mM NaCl, 125 mM imidazole, and 2 mM dithiothreitol). The protein concentration was measured using the Bradford assay, and the activity was assayed using mixed micelles in the modified Dole assay (31, 32). Purified GIVA PLA_2 (2 mg/ml) was stored in the protein buffer on ice for DXMS experiments (16).

Preparation of Deuterated Samples—D_2O buffer contained 50 mM HEPES (pH 6.9), 100 mM NaCl, 2 mM dithiothreitol, ($\pm$) 200 μM $CaCl_2$. Hydrogen/deuterium exchange experiments were initiated by mixing 20 μl of GIVA PLA_2, the C2 domain, or the catalytic domain (containing 40 μg) in protein buffer with 60 μl of D_2O buffer to a final concentration of 70.4% D_2O at pH 7.0. In calcium binding experiments, the GIVA PLA_2 in protein buffer was preincubated in the presence of 240 μM $CaCl_2$ in a 23 °C water bath for 5 min. The D_2O buffer was then added, and the samples were incubated at 23 °C for an additional 10 s, 30 s, 100 s, 300 s, 1000 s, 3000 s, or 200 min. Each time point of the intact GIVA PLA_2 was repeated three independent times. The deuterium exchange was quenched by adding 120 μl of ice-cold quench solution (0.96% formic acid, 1.66 M guanidine hydrochloride) that acidified the sample to a final pH 2.5. The samples were placed on ice at the quenched condition for 10 min to partially denature the protein for the purpose of better peptide map coverage and then frozen on dry ice. Fully deuterated samples were incubated in 2.5 M guanidine hydrochloride, 75% D_2O at 23 °C for 2 days. Vials with frozen samples were stored at −80 °C until analysis, usually within 3 days.

Proteolysis Liquid Chromatography-Mass Spectrometry Analysis of Samples—All steps were performed at 0 °C as previously described (26, 28). The samples were hand-thawed on melting ice and injected onto and passed through a protease column (66-μl bed volume) filled with porcine pepsin (Sigma; immobilized on Poros 20 AL medium at 30 mg/ml following the manufacturer's instructions, Applied Biosystems) at a flow rate of 100 μl/min with 0.05% trifluoroacetic acid. The eluate from the pepsin column was directly loaded onto a C18 column (Vydac cat. 218MS5150). The peptides were eluted at 50 μl/min with a linear gradient of 0.046% trifluoroacetic acid, 6.4% (v/v) acetonitrile to 0.03% trifluoroacetic acid, 38.4% acetonitrile for 30 min. The eluate from the C18 column was directed to a Finnigan Classic LCQ mass spectrometer via its ESI probe operated with a capillary temperature of 200 °C as previously described (26, 28).

Data Processing—SEQUEST software (Thermo Finnigan Inc.) was used to identify the sequence of the peptide ions. DXMS Explorer (Sierra Analytics Inc, Modesto CA) was used for the analysis of the mass spectra as previously described (26, 28). All selected peptides had first passed the quality control threshold of the software and were then manually checked for the mass envelope fitting with the calculated mass envelope for data reduction. The highest signal/noise ion was picked if multiple ionization charges (1, 2, or 3) of a peptide were detected. Normally, the peptide with the lower charge gave a better signal. Incorporated deuteron number was the centroid shift between the non-deuterated and the partially deuterated mass envelope. The deuteration level of each peptide was calculated by the ratio of the incorporated deuteron number to the maximum possible deuteration number.

RESULTS

GIVA PLA_2 Coverage Map of Pepsin Fragmentation—The protein digestion procedure was optimized to produce a peptide map that yielded the best coverage of GIVA PLA_2. These optimizations included testing various denaturants and denaturing conditions, denaturation times, amounts of protein, and flow rates for the online pepsin digestion. The final method is described under "Experimental Procedures." The optimized condition gave a 92% coverage of the GIVA PLA_2 sequence with 157 distinct peptic peptides being identified, see Fig. 1. The C2 domain and the catalytic domain alone generated the same digestion pattern as their respective parts did in the intact GIVA PLA_2. There are 58 unresolved amino acid residues. These are due to regions without identified peptides and the fact that the first two residues of each peptide are rapidly exchanging and do not retain deuterons during the processing. Although we analyzed all 157 peptides, some regions of the protein contained several overlapping peptides. In some cases, comparing the deuterium levels of overlapping peptides will yield information about the deuterium levels of a subsection of the peptide. Thus, one can obtain information about regions of the protein smaller than the peptides covering it. In many cases, however, the orientation of the overlapping peptides is such that no additional information can be obtained. Also, in some

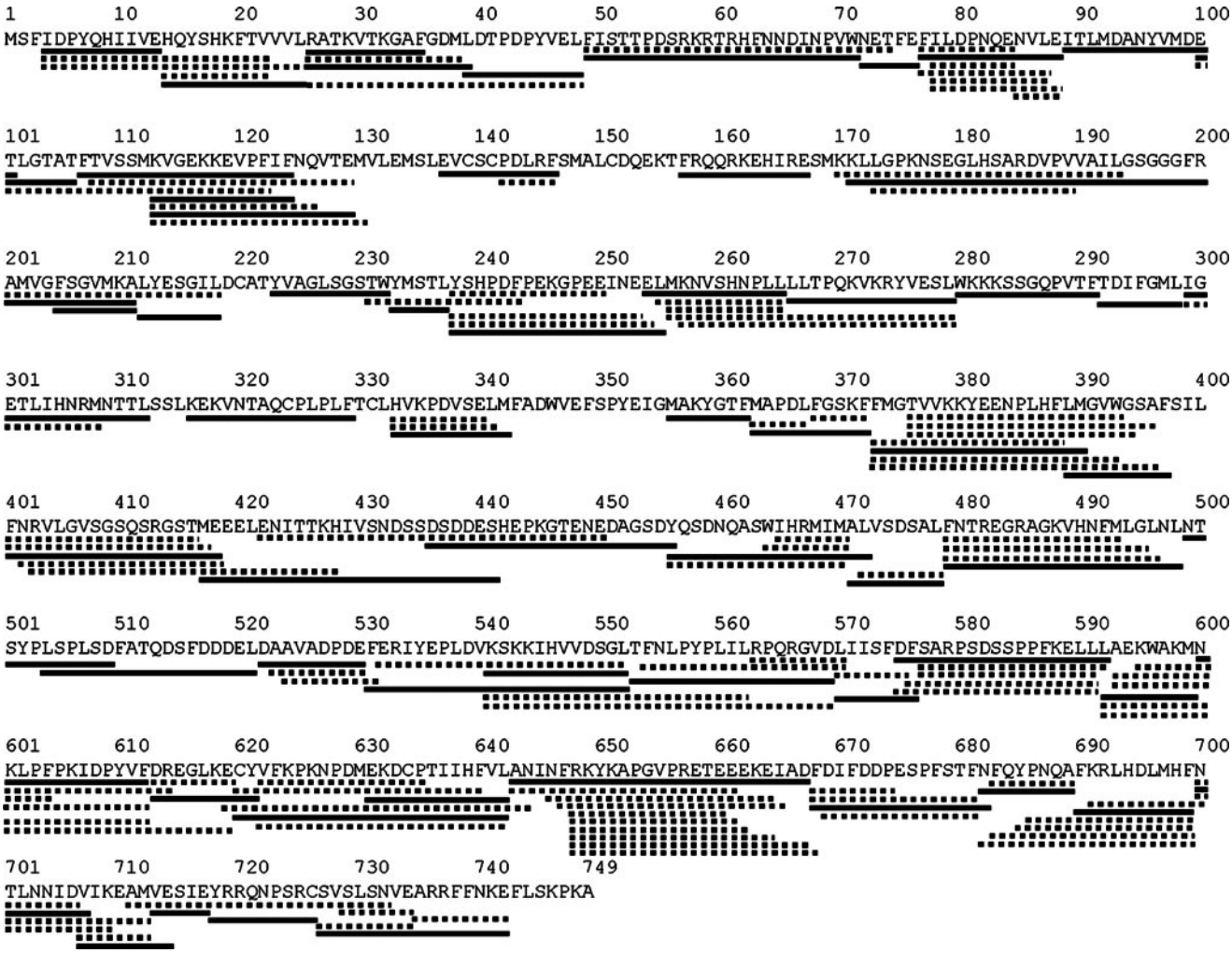

FIGURE 1. **Pepsin-digested peptide coverage map of GIVA PLA_2.** Identified and analyzed peptides resulting from pepsin digestion are shown *below* the primary sequence of GIVA PLA_2. Only the peptides shown as *solid lines* were used in this study.

cases, the error propagation through these calculations yields large variances that prevent further analysis. Because of these latter two reasons, peptides that could not provide additional information were eliminated. In the end, 59 peptide fragments, which cover 82% of the protein, were employed. In this article, when we use the term "peptide," we are referring to an actual peptide that was identified in the pepsin digestion. When we use the term "region," we are referring to a section of the protein for which the deuterium exchange has been calculated but may or may not correspond to an actual pepsin peptide.

Deuterium On-exchange of GIVA PLA_2—Full deuteration was also tried under various conditions such as 2 days of exchange in 0.5% formic acid, high temperature exchange for 4 h (50 °C), and partial denaturation in 2.5 M guanidine hydrochloride. The resulting low deuteration observed for the α/β hydrolase region indicated that the protein was not fully deuterated under all conditions. The peptide fragment 266–279 containing a solvent-exposed loop-helix structure had the highest deuteration level (89%). Hence, this peptide was used as a system back-exchange control. Back-exchange (12%) according to the fully deuterated control and the deuteration level (70.4%) was corrected for the centroid shifts.

Deuterium on-exchange experiments of GIVA PLA_2 (±) Ca^{2+} were incubated at pH 7.0, 23 °C for seven different time points ranging from 10 s to 200 min and were processed as described above. Under these conditions of temperature, pH, and time, the deuteration levels of the peptides were well distributed between 3 and 90%, and there was a 12% back-exchange. The deuteration level after deuterium on-exchange over the time course is shown in Fig. 2. Fig. 1 shows the actual physical peptides that were isolated, detected, and analyzed via DXMS. Fig. 2 shows the deuterium exchange levels of various regions of the protein, not the peptides *per se*. The presence of overlapping peptides in Fig. 1 allows one to define the deuteration level of regions of the protein smaller than the peptides by comparing the deuterium levels of several overlapping peptides. Note that the first two N-terminal residues of each pepsin-digested DXMS peptide do not retain deuterium after the pepsin and C18 columns; this fact is also taken into account when calculating the deuteration levels of the protein regions shown in Fig. 2 (28, 33).

The deuteration level after 3000 s on-exchange was plotted onto the GIVA PLA_2 structure (Protein data bank code 1cyj) using a color index to illustrate the H/D exchange results for the

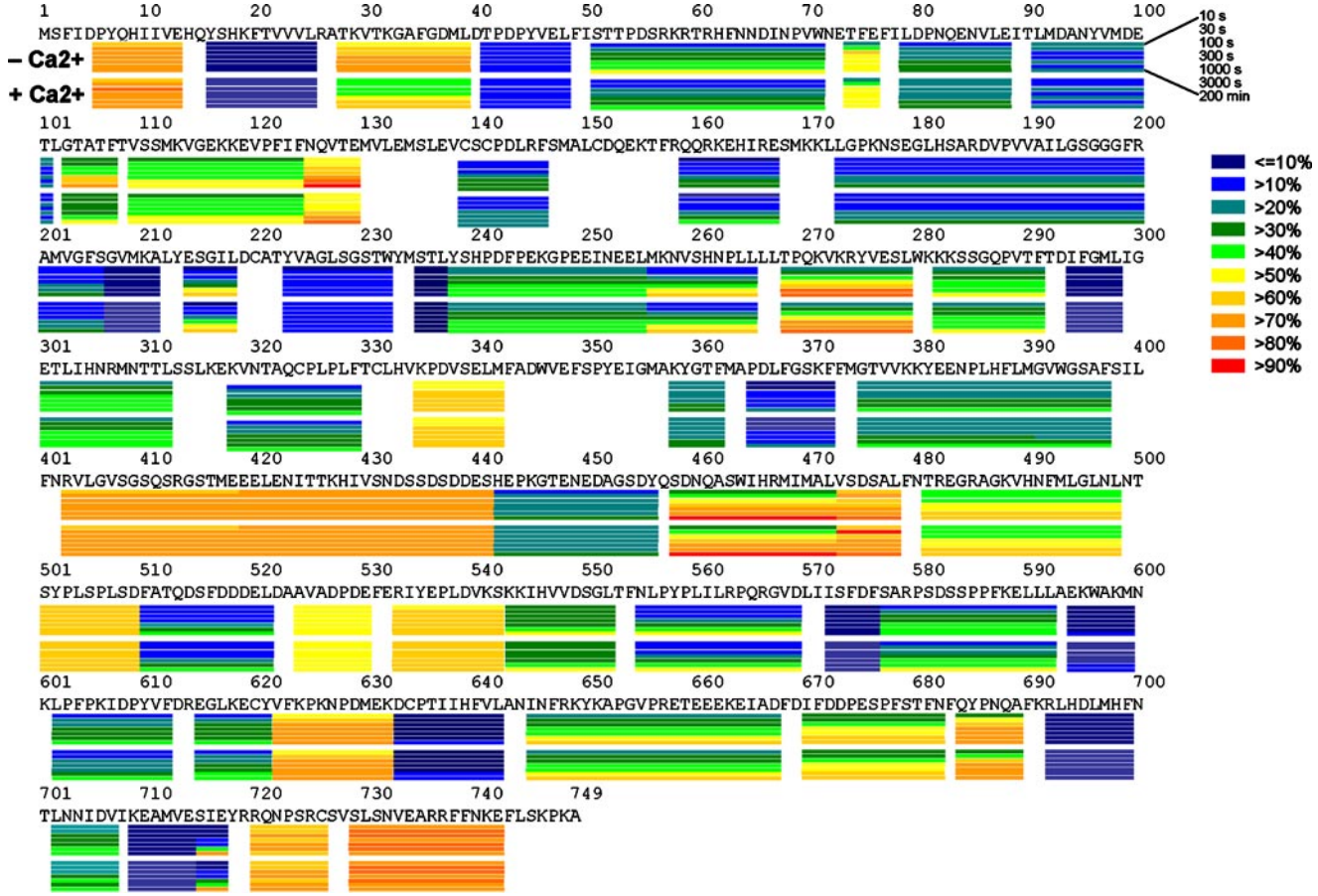

FIGURE 2. **Deuterium exchange of the GIVA PLA_2 in the presence and absence of Ca^{2+}.** There are two main sets of *colored bars*, one for exchange with Ca^{2+} and one without Ca^{2+}. Each bar is divided into rows corresponding to each time point from 10 s to 200 min (*top* to *bottom*). The *color coding* indicates the percent of H/D exchange in the given time period.

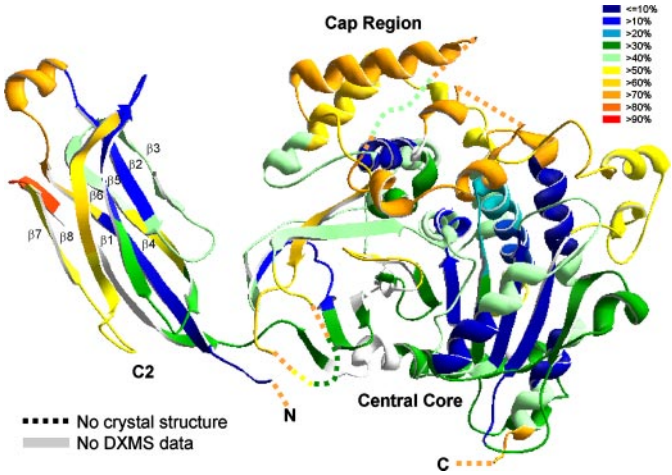

FIGURE 3. **Deuteration level of GIVA PLA_2.** The deuterium exchange map of GIVA PLA_2 is shown after 3000 s of on-exchange, with the *color coding* indicating the percentage of H/D exchange. There are five regions in the protein for which there is no crystal structure information, and these regions are shown by a *dashed line*. The *line color* indicates the exchange rates detected by DXMS, but the position and length of these *dashed lines* are not based upon any structural information and were added simply to show the DXMS data.

structure as shown in Fig. 3. The C2 domain consists of 8 antiparallel β-strands that are roughly divided into two domains. The first contains the β6-, β7-, and part of the β8-strands (which includes residues 6–13, 28–39, 73–76, and 125–129) and exhibits fast deuterium exchange. The second domain contains β1-, β2-, and β5-strands (which include residues 16–25, 41–48, and 91–101) and exhibits slow H/D exchange. The fast exchanging regions of the C2 domain tend to face away from the catalytic domain. The slow exchanging regions are on the opposite side of the C2 domain and face the cleft between the C2 and catalytic domains. The crystal structure indicates that there is a significant amount of open space between these two domains, but of course the crystallographic data reflect the crystal packing rather than the solution conformation. This would predict that there would be significant accessibility of water to the internal face of the C2 domain, see Fig. 3. The slow exchange in this region of the C2 domain could be due to the rigidity of the protein structure here, or it could be due to the fact that when free in solution, the C2 domain is folded against the catalytic domain.

There are five regions in the x-ray crystal structure that could not be resolved because of the flexibility of the chains. These are indicated in Fig. 3 as dashed lines. It should be noted, that the DXMS method was able to detect and measure H/D exchange in each of these regions. As expected, these regions showed significant levels of exchange. Two of these regions are the hinges for the catalytic site lid (22).

The catalytic domain contains a cap region (residues 370–548), a central core (residues 139–369 and 549–719), and a C-terminal tail (residues 720–742). The cap region contains a

high percentage of fast exchanging residues. They include residues 403–441, 458–478, 501–509, and 524–542. The lid (residues 413–457) in the cap region that regulates the active site also shows fast exchange. The central core contains two regions (335–342 and 622–632) that show fast exchange. Most of the α/β central core exhibits slow exchange (residues 207–211, 223–237, 294–298, 365–371, 572–576, 594–599, 633–642, 692–699, and 709–714). The C terminus (residues 720–742) and N terminus also exhibit fast exchange.

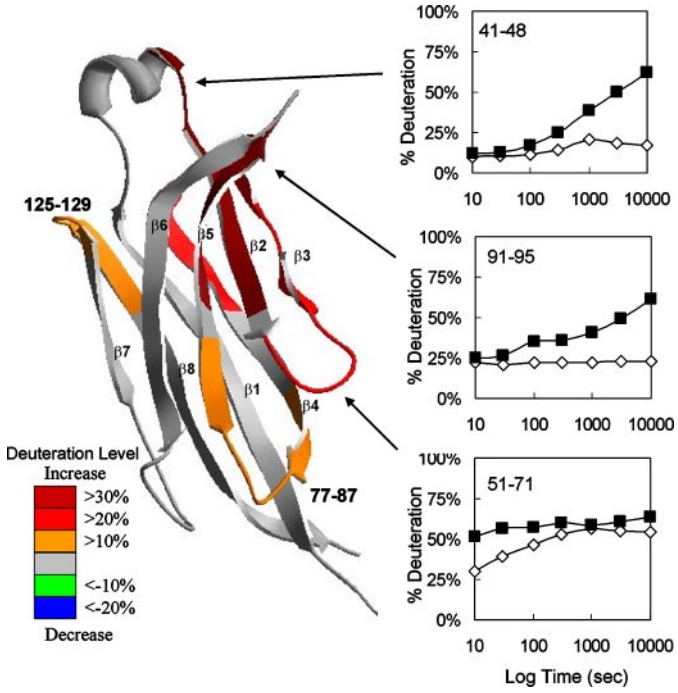

FIGURE 4. **Differences in the deuteration level of the C2 domain alone in comparison to the C2 domain in the intact GIVA PLA$_2$.** The percentage of deuteration at seven time points showed a maximum of over 20% increase in three regions in *red* (residues 41–48, 91–95, and 51–71) of the C2 domain alone (■) over the C2 domain in the intact GIVA PLA$_2$ (◇). The regions in *orange* showed a maximum of 10–20% increases and are labeled with the residue number.

Deuterium On-exchange of the C2 Domain and the Catalytic Domain of GIVA PLA$_2$—To test the hypothesis that there is a dynamic interaction between the C2 domain and the catalytic domain, we expressed and purified His$_6$-tagged C2 and His$_6$-tagged catalytic domains individually and conducted DXMS experiments on both under the same conditions as the intact GIVA PLA$_2$. The differences in the deuteration level between the C2 domain alone and the intact GIVA PLA$_2$ are shown in Fig. 4. The C2 domain alone showed greater than a 20% increase of solvent accessibility (residues 41–48, 91–95, and 51–71) on β2, β3, β4, and β5 in the cleft. Most regions in β1, β6, β7, and β8 outside of the cleft were unchanged, except for region 125–129, which was the only one showing a greater than 10% increase, but it was not significant after 100 s. This result indicates that the catalytic domain either interacts with the C2 domain or it changes the conformation of the C2 domain through the linker region, leading to an increase in its solvent accessibility (Fig. 4).

To find out if the increase in the solvent accessibility of the C2 domain is through the contact with the catalytic domain, we carried out hydrogen/deuterium exchange on the isolated catalytic domain (Fig. 5). The DXMS of the catalytic domain showed over a 20% increase in the region of residues 363–372, 373–388, 389–397, and 494–498 in the cleft. Also, several regions in the cap (residues 254–265, 266–279, 280–291, 292–298, 479–495, and 541–553) showed a 10–20% increase. The effect of the C2 domain on the catalytic domain is much more than the linker region and the contact region next to the linker region shown in the crystal structure, which indicates a more extensive interaction between the two domains. When we mixed the C2 domain and the catalytic domain in a 1:1 molar ratio for DXMS, the result was the same as running them individually (data not shown.) No evidence for an interaction between the two domains was observed. Clearly, the linker region is necessary for the interaction between the C2 and catalytic domains.

Comparison of the DXMS results of the C2 domain and the catalytic domain alone to the intact GIVA PLA$_2$ allowed us to localize where the C2 domain interacts with the catalytic domain. This result supports the hypothesis that there is an interaction between the C2 and the

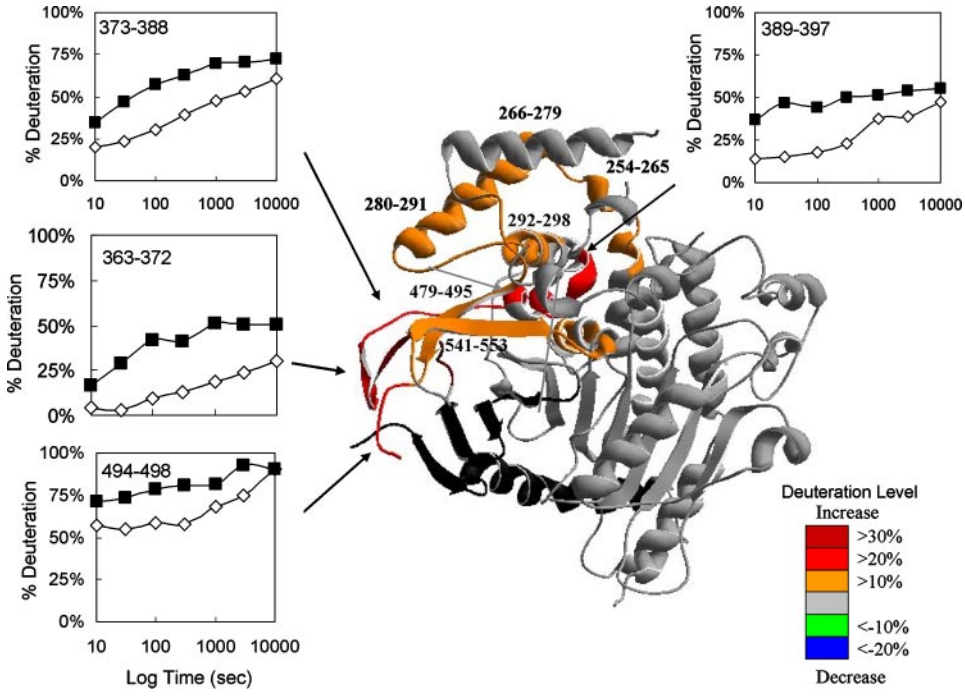

FIGURE 5. **Differences in the deuteration level of the catalytic domain alone in comparison to the catalytic domain in the intact GIVA PLA$_2$.** The percentage of deuteration at seven time points showed a maximum of over 20% increases in four regions in *red* (residues 363–372, 373–388, 389–397, and 494–498) of the catalytic domain alone (■) over the catalytic domain in the intact GIVA PLA$_2$ (◇). The regions in *orange* showed a maximum of 10–20% increases and are labeled with the residue number. The area in *black* has no DXMS data.

catalytic domain and allowed us to map out the interaction regions between them.

Calcium Binding Effects on GIVA PLA_2—The Ca^{2+}-binding site on GIVA PLA_2 consists of the three distinct Ca^{2+}-binding loops CBL1, CBL2, and CBL3. This region has been shown to be important for lipid interface binding with the CBL1 and CBL3 regions playing a dominant role (23, 34, 35). We carried out the on-exchange in the presence and absence of 200 μM Ca^{2+}. We first examined the residues that directly interact with Ca^{2+}. The two Ca^{2+} ions coordinate with Asp-40, Thr-41, and Asp-43 in CBL1, with Asn-65 in the CBL2 region, and Asp-93, Ala-94, and Asn-95 in CBL3. Thr-41 and Asp-43 in CBL1 exhibit slow exchange in the absence of Ca^{2+} (Fig. 6). There was only an additional 5% decrease in H/D exchange at 200 min when Ca^{2+} was bound. Residue Asp-40 in CBL2 is in a gap between two resolved DXMS peptides, and thus we have no H/D exchange information for this residue. Asp-93, Ala-94, and Asn-95 in CBL3 are located in the DXMS peptide 91–101, and this peptide exhibited only a 10% H/D exchange after 200 min without Ca^{2+}. Its exchange rate did not change with Ca^{2+}. Asn-65 in CBL2 is the only residue that is located on a DXMS peptide that showed a 10% decrease in H/D exchange upon Ca^{2+} binding (see Fig. 6). However, the resolution in this region was not sufficient to assign the H/D exchange changes to Asn-65.

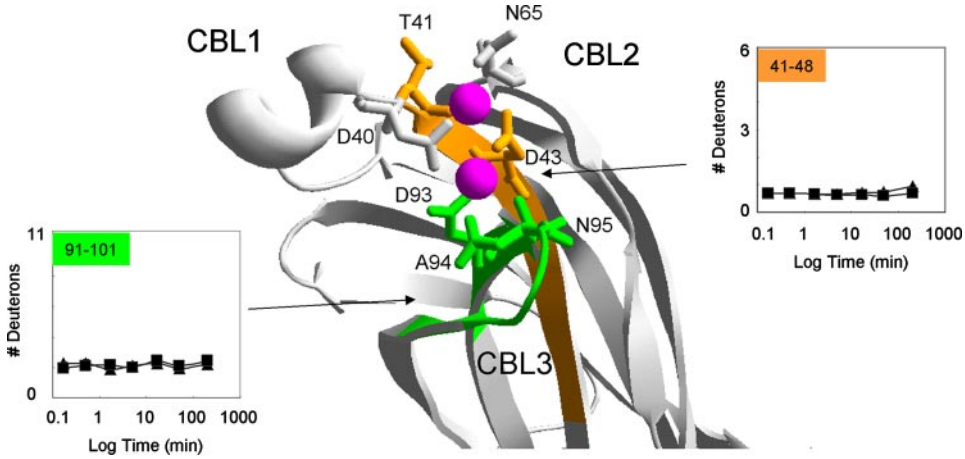

FIGURE 6. **Deuterium exchange in the Ca^{2+}-binding site of the C2 domain.** The number of incorporated deuterons at seven time points in two regions, 41–48 and 91–101 of the C2 domain of the intact GIVA PLA_2, are plotted in the presence (■) and absence of Ca^{2+} (▲). The calcium-binding residues are shown in *stick representation*. In the figure, the region in *green* corresponds to residues 91–101, and the region in *orange* corresponds to residues 41–48. The *error bars* are based on the standard deviation of triplicates.

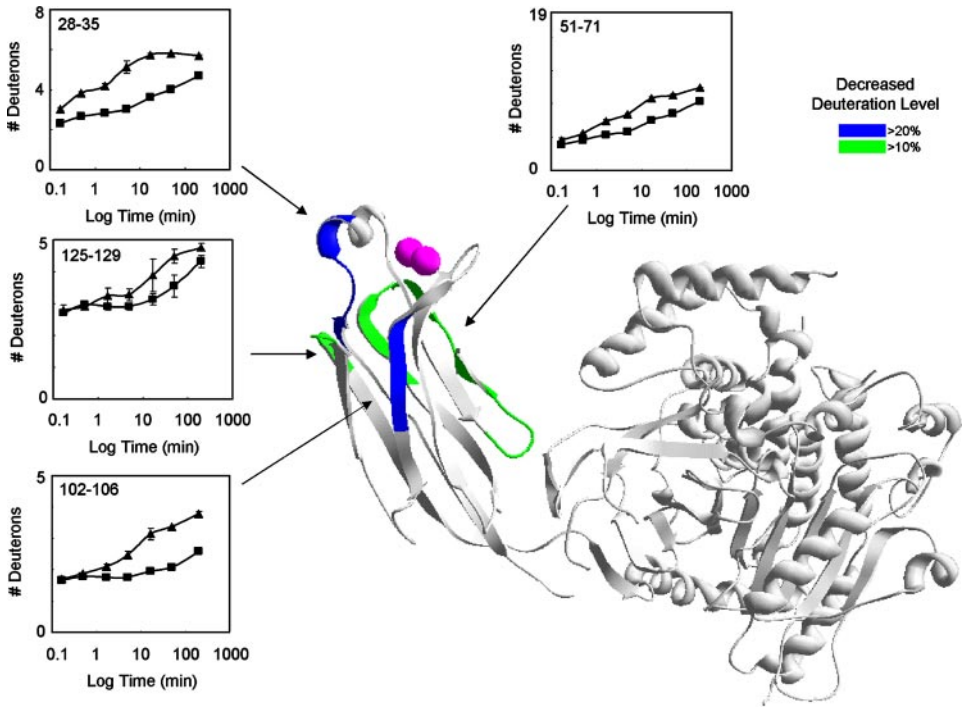

FIGURE 7. **Ca^{2+} binding effects on deuterium exchange of the intact GIVA PLA_2.** The number of incorporated deuterons in the C2 domain of GIVA PLA_2 in the presence (■) and absence of Ca^{2+} (▲) are shown for regions in which deuterium exchange decreased upon Ca^{2+} binding as indicated in *green* or *blue* on the structural diagram. The decreased percentage of deuteration mapped onto the GIVA PLA_2 structure was calculated by taking the average of the last three time points shown in the plots. The two calcium ions are shown in *pink*. The *error bars* are based on the standard deviation of triplicates.

There were, however, dramatic changes in other areas of the C2 domain that indicated a conformational change in the protein. Four regions in the C2 domain had a significantly decreased H/D exchange rate; these were residues 26–39, 51–71, 102–106, and 125–129. The incorporated deuterium number over the time course in these four regions is plotted in Fig. 7. The average change in deuteration level of the FOUR time points from 5–200 min were also mapped onto the GIVA PLA_2 structure in the same figure.

Residues 28–35 on CBL1 exhibited a 22% decrease in deuteration levels upon Ca^{2+} binding. We have four DXMS peptides that cover the region from 26–39, including 26–35, 26–38, 26–39, and 26–48. All four peptides showed between a 1 and 2 deuteron decrease after Ca^{2+} binding. By comparing the H/D exchange of the peptides 26–35, 26–38, and 26–39, we determined that the protein region 36–39 is not affected by calcium binding and retained about 3 deuterons that accounts for 75–80% deuteration. Interestingly, residues 28–35 decreased the incorporation of 2 deuterons caused by binding of Ca^{2+}.

Two DXMS peptides, 49–71 and 49–74 containing CBL2, showed an 11% deuteration level decrease upon Ca^{2+} binding in this region. Residues 102–106, which are next

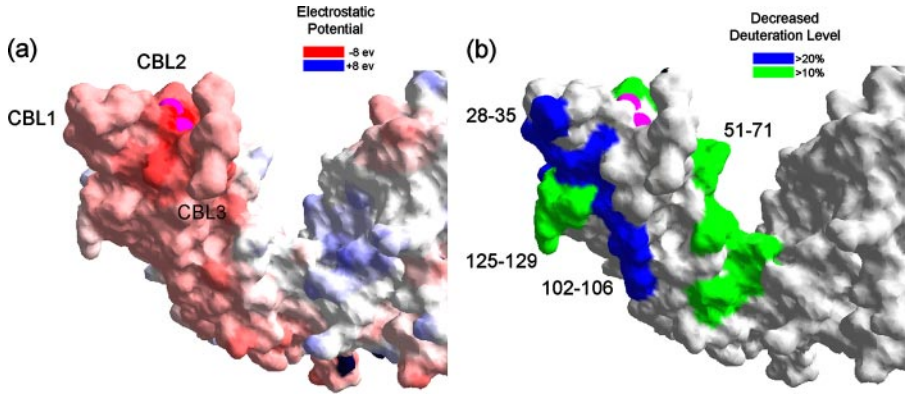

FIGURE 8. **The electrostatic potential and the decreased deuteration level of the C2 domain in the intact GIVA PLA_2.** *a*, the electrostatic potential mapped to the molecular surface is calculated by Swiss-Pdb Viewer 3.7, based on the simple coulomb interaction. *b*, the decreased deuteration level is mapped to the molecular surface with the same orientation as the electrostatic potential.

to CBL3, showed a 22% deuteration level decrease upon Ca^{2+} binding. Comparing DXMS peptides 115–129 and 115–124 showed that protein residues 125–129 on the β6-β7 loop showed a 13% deuteration level decrease upon Ca^{2+} binding.

We also examined H/D exchange levels on the rest of the protein and found no significant change in the H/D exchange levels in the catalytic domain. It is worth noting that the linker region (residues 139–146) showed a 6% solvent accessibility decrease upon calcium binding, which suggests minor interaction or orientation changes between the C2 and the catalytic domain.

DISCUSSION

DXMS results provide a detailed H/D exchange rate profile of the catalytic domain. The crystal structure of the GIVA PLA_2 contains a lid in the cap region that is tethered to the rigid catalytic core by two very flexible peptides and that blocks the catalytic site in the crystal structure. The lid apparently must move out of the way so that substrate can bind to the catalytic site. It has also been suggested that the cap is involved in membrane association (24). Our deuterium exchange results are consistent with these hypotheses. The lid and the tethers on either side of it show fast exchange. Interestingly, the deuterium DXMS method was able to detect and measure the exchange of the two tethers that could not be seen via x-ray crystallography and have confirmed that they have fast exchange. These results are consistent with the hypothesis that the lid is a flexible regulatory structure that can move when the enzyme interacts with lipid interfaces to expose the active site in the rigid catalytic domain.

The GIVA PLA_2 has been shown to translocate to the Golgi and perinuclear regions of cells upon the release of Ca^{2+} (36–38). This movement has been suggested to be one important way for the cell to control the action of this enzyme and eicosanoid production. The C2 domain is clearly responsible for this action. The Ca^{2+}-dependent membrane docking of the C2 domain alone of this and many other proteins has been extensively studied to understand how its structure affects membrane penetration and the sequestration of the enzyme at the lipid surface. It is believed that the C2 domain allows the GIVA PLA_2 to bind to the membrane and that it positions the active site in a way that facilitates the binding of the substrate. Two Ca^{2+} ions coordinate with Asp and Asn residues in the anion hole on the tip of the C2 domain to neutralize negative charges in this region. The hydrophobic residues on the tip of CBL1 (Phe-35, Met-38, and Leu-39) and CBL3 (Tyr-96, Val-97, and Met-98) interact with the hydrophobic phospholipid headgroup (21). After the binding to the phospholipid bilayer, the dissociation rate of Ca^{2+} decreases (39, 40). Ca^{2+} binding may cause a conformational change of the C2 domain, which effectively hides the hydrophilic residues and exposes the hydrophobic residues.

One of the most dramatic differences that we observed occurred in the C2 domain. The surface of the C2 domain that faces away from the catalytic domain showed significant H/D exchange, whereas the opposite surface that faces the catalytic domain showed slow exchange. H/D exchange rates are affected by accessibility to water and can reflect the rigidity of the protein secondary structure and the strength of the hydrogen bonds. Both of these regions are composed of antiparallel β-sheets, and one might expect that they would have the same structural characteristics, and thus the H/D exchange rates would be similar. The decreased exchange on the surface facing the catalytic domain could be due to the fact that in solution the C2 domain rests up against the catalytic domain, and thus water accessibility is decreased. The slow exchange regions in the cleft between the C2 domain and the catalytic domain had over a 20% increase of the solvent accessibility when we conducted the DXMS experiments on the C2 domain or the catalytic domain alone. This would imply that the cleft delineated in the x-ray structure is in a different orientation of the protein when there is no calcium binding. It should be noted that the C2 and catalytic domains are held together by a single short peptide linker that should be fairly flexible. The interaction or the contact regions between the C2 domain and the catalytic domain can be mapped out by the solvent accessibility difference of the two individual domains and the intact GIVA PLA_2 (Figs. 4 and 5).

To compare the effects of calcium binding on structural perturbations and charge neutralization, the electrostatic potential and the Ca^{2+} binding effects measured by DXMS were plotted onto the molecular model of GIVA PLA_2 (Fig. 8). The anion hole surrounded by CBL1, CBL2, and CBL3 on the top of the C2 domain is highly negatively charged. The cleft between the C2 and catalytic domains has a low to positive electrostatic potential (Fig. 8*a*). We also showed low solvent accessibility of the β2 and β5 sheets (Fig. 3). The linker region between the C2 domain and the catalytic domain is possibly a flexible loop, because the regions 132–136 and 147–156 may be overdigested by pepsin and were not covered in the peptide map (Fig. 1). This evidence suggests that the C2 domain is probably in physical contact with the catalytic domain. Additionally, the two Ca^{2+} ions

bind directly to the anion hole to neutralize the negative charge (Fig. 8*a*).

We observe the largest change in electrostatics in the anion hole; however, the overall decreased H/D exchange regions do not occur in this region (Fig. 8*b*). The most significantly decreased regions are on either side of the anion hole. Fig. 6 shows that the regions that directly bind Ca^{2+} have very slow exchange that did not change upon calcium binding. This suggests that the anion hole has either a low D_2O accessible/exchanging location or is very rigid. On the other hand, the surfaces surrounding the anion hole showed more exchange without calcium and showed decreased H/D exchange rates upon calcium binding. Both the C2 surface facing away from the catalytic site and the surface facing it showed decreased H/D exchange upon Ca^{2+} binding. Because both of these surfaces have a decreased exchange and there is nothing on the outside surface that would hinder access to water, we conclude that the observed effects are due to Ca^{2+} tightening up the pleated sheet structure in these regions and thus stabilizing the hydrogen bonds. CBL1 and CBL3 are both components of the anion hole. These two loops show slow exchange on the side of the anion hole and fast exchange on the molecular surface. These results are consistent with the proposed membrane penetration model (24) and indicate that the conformational change and negative charge neutralization occurs immediately after Ca^{2+} binding.

In conclusion, DXMS has allowed us to observe the interaction between the C2 domain and the catalytic domain and the effects of Ca^{2+} binding on the intact GIVA PLA_2 from a unique perspective. The C2 domain shows extensive interaction with the catalytic domain beyond the linker region. While the calcium binding effects are mainly on the C2 domain, Ca^{2+} binding may extend its effects and have implications for the catalytic domain. Binding of two Ca^{2+} ions cause a conformational change on the C2 domain, tightening up the regions surrounding the anion hole. The rigidified conformation of the C2 domain constitutes an initial step leading to enzyme interfacial activation, but this work shows clearly that changes in the cap and lid of the catalytic domain also play a critical role in enzyme interactions and the full catalytic activity of the enzyme.

REFERENCES

1. Kramer, R. M., Roberts, E. F., Manetta, J., and Putnam, J. E. (1991) *J. Biol. Chem.* **266,** 5268–5272
2. Clark, J. D., Lin, L. L., Kriz, R. W., Ramesha, C. S., Sultzman, L. A., Lin, A. Y., Milona, N., and Knopf, J. L. (1991) *Cell* **65,** 1043–1051
3. Schaloske, R. H., and Dennis, E. A. (2006) *Biochim. Biophys. Acta* **1761,** 1246–1259
4. Six, D. A., and Dennis, E. A. (2000) *Biochim. Biophys. Acta* **1488,** 1–19
5. Goetzl, E. J., An, S., and Smith, W. L. (1995) *Faseb J.* **9,** 1051–1058
6. Kramer, R. M., and Sharp, J. D. (1995) *Agents Actions Suppl.* **46,** 65–76
7. Funk, C. D. (2001) *Science* **294,** 1871–1875
8. Lucas, K. K., Svensson, C. I., Hua, X. Y., Yaksh, T. L., and Dennis, E. A. (2005) *Br. J. Pharmacol.* **144,** 940–952
9. Sapirstein, A., and Bonventre, J. V. (2000) *Biochim. Biophys. Acta* **1488,** 139–148
10. Alonso, F., Henson, P. M., and Leslie, C. C. (1986) *Biochim. Biophys. Acta* **878,** 273–280
11. Seilhamer, J. J., Pruzanski, W., Vadas, P., Plant, S., Miller, J. A., Kloss, J., and Johnson, L. K. (1989) *J. Biol. Chem.* **264,** 5335–5338
12. Nalefski, E. A., Sultzman, L. A., Martin, D. M., Kriz, R. W., Towler, P. S., Knopf, J. L., and Clark, J. D. (1994) *J. Biol. Chem.* **269,** 18239–18249
13. Lin, L. L., Wartmann, M., Lin, A. Y., Knopf, J. L., Seth, A., and Davis, R. J. (1993) *Cell* **72,** 269–278
14. Kramer, R. M., Roberts, E. F., Um, S. L., Borsch-Haubold, A. G., Watson, S. P., Fisher, M. J., and Jakubowski, J. A. (1996) *J. Biol. Chem.* **271,** 27723–27729
15. Das, S., Rafter, J. D., Kim, K. P., Gygi, S. P., and Cho, W. (2003) *J. Biol. Chem.* **278,** 41431–41442
16. Six, D. A., and Dennis, E. A. (2003) *J. Biol. Chem.* **278,** 23842–23850
17. Mosior, M., Six, D. A., and Dennis, E. A. (1998) *J. Biol. Chem.* **273,** 2184–2191
18. Stahelin, R. V., Subramanian, P., Vora, M., Cho, W., and Chalfant, C. E. (2007) *J. Biol. Chem.* **282,** 20467–20474
19. Subramanian, P., Stahelin, R. V., Szulc, Z., Bielawska, A., Cho, W., and Chalfant, C. E. (2005) *J. Biol. Chem.* **280,** 17601–17607
20. Xu, G. Y., McDonagh, T., Yu, H. A., Nalefski, E. A., Clark, J. D., and Cumming, D. A. (1998) *J. Mol. Biol.* **280,** 485–500
21. Perisic, O., Fong, S., Lynch, D. E., Bycroft, M., and Williams, R. L. (1998) *J. Biol. Chem.* **273,** 1596–1604
22. Dessen, A., Tang, J., Schmidt, H., Stahl, M., Clark, J. D., Seehra, J., and Somers, W. S. (1999) *Cell* **97,** 349–360
23. Bittova, L., Sumandea, M., and Cho, W. (1999) *J. Biol. Chem.* **274,** 9665–9672
24. Das, S., and Cho, W. (2002) *J. Biol. Chem.* **277,** 23838–23846
25. Mandell, J. G., Falick, A. M., and Komives, E. A. (1998) *Proc. Natl. Acad. Sci. U. S. A.* **95,** 14705–14710
26. Hamuro, Y., Anand, G. S., Kim, J. S., Juliano, C., Stranz, D. D., Taylor, S. S., and Woods, V. L., Jr. (2004) *J. Mol. Biol.* **340,** 1185–1196
27. Hoofnagle, A. N., Resing, K. A., Goldsmith, E. J., and Ahn, N. G. (2001) *Proc. Natl. Acad. Sci. U. S. A.* **98,** 956–961
28. Brudler, R., Gessner, C. R., Li, S., Tyndall, S., Getzoff, E. D., and Woods, V. L., Jr. (2006) *J. Mol. Biol.* **363,** 148–160
29. Hochrein, J. M., Lerner, E. C., Schiavone, A. P., Smithgall, T. E., and Engen, J. R. (2006) *Protein Sci.* **15,** 65–73
30. Engen, J. R., and Smith, D. L. (2001) *Anal. Chem.* **73,** 256A–265A
31. Lucas, K. K., and Dennis, E. A. (2005) *Prostaglandins Other Lipid Mediat.* **77,** 235–248
32. Yang, H. C., Mosior, M., Johnson, C. A., Chen, Y., and Dennis, E. A. (1999) *Anal. Biochem.* **269,** 278–288
33. Bai, Y., Milne, J. S., Mayne, L., and Englander, S. W. (1993) *Proteins* **17,** 75–86
34. Perisic, O., Paterson, H. F., Mosedale, G., Lara-Gonzalez, S., and Williams, R. L. (1999) *J. Biol. Chem.* **274,** 14979–14987
35. Malkova, S., Long, F., Stahelin, R. V., Pingali, S. V., Murray, D., Cho, W., and Schlossman, M. L. (2005) *Biophys. J.* **89,** 1861–1873
36. Gijon, M. A., Spencer, D. M., Kaiser, A. L., and Leslie, C. C. (1999) *J. Cell Biol.* **145,** 1219–1232
37. Glover, S., de Carvalho, M. S., Bayburt, T., Jonas, M., Chi, E., Leslie, C. C., and Gelb, M. H. (1995) *J. Biol. Chem.* **270,** 15359–15367
38. Channon, J. Y., and Leslie, C. C. (1990) *J. Biol. Chem.* **265,** 5409–5413
39. Corbin, J. A., Evans, J. H., Landgraf, K. E., and Falke, J. J. (2007) *Biochemistry* **46,** 4322–4336
40. Nalefski, E. A., Slazas, M. M., and Falke, J. J. (1997) *Biochemistry* **36,** 12011–12018